Incipient Instability of Growth in Blends of Polymer Melts

S. Balijepalli and J. M. Schultz*

Department of Chemical Engineering, University of Delaware, Newark, Delaware 19716

Received June 26, 1995; Revised Manuscript Received November 30, 1995[⊗]

ABSTRACT: Crystallization from melts of polymer blends containing a noncrystallizable component (solute) results in morphologies that are "open", based upon bundles of lamellas separated from one another by noncrystalline regions. We model the formation of an open spherulite initially as growth of a compact sphere. The growing sphere rejects the noncrystallizable component (solute). To allow for better dissipation of the solute, the interface breaks down into protuberances, the result being the transition of a compact sphere to a more open one. The stabilizing effects are the kinetics of attachment and the capillarity effect at the interface. The balance between the breakdown and stabilization determines the critical radius of instability (R_r) of a growing sphere. We have computed R_r from a stability analysis which includes the Lauritzen and Hoffman interface kinetics for the crystallizing species. Results for a blend of isotactic polystyrene and atactic polystyrene indicate that there exists a sharp transition from relatively large stable spheres to unstable ones, over a few degree of undercooling. R_r's predicted for undercoolings of 25 K and higher are in the submicrometer range. The value of R_r provides an upper bound for the bundle diameter. The predictions for the i-PS/a-PS blend are consistent with experimentally observed results: the bundle diameter is in the submicrometer range for large undercoolings and changes little with undercooling, the diameter being in the range of 0.06−0.02 μm (∼2−6 lamellas/bundle) for an undercooling of 35−55 K.

Introduction

Polymers undergoing phase transformation show a wide variety of microstructures. The most common growth form observed is termed "spherulitic". This form consists of radial arrays of predominantly chain folded crystals which are lamellar. Several aspects of the formation of spherulites are not well understood, particularly the early evolution of the structure and the subsequent noncrystallographic branching of the chain-folded crystals. Our purpose in this section is to outline some views regarding the early stages of growth. An early review by Passaglia and Khoury[1] presents several salient morphological features of spherulitic growth. The formation of spherulites occurs through a series of stages. In the first stage, multilayered chain-folded structures, sheaflike in appearance, are formed either by additional chain-folded layers developing on a single crystal or by simultaneous formation of several lamellas.[2] The constituent layers gradually fan out or splay progressively as sketched in Figure 1. Further evolution of these structures (referred to as axialites/hedrites) into three-dimensional spherulites occurs by continued splaying of lamellas along more than one axis. Careful work on the crystallization of narrow fractions of homopolymers (polyethylene and poly(ethylene oxide)) by Mandelkern[3,4] indicates that the formation of spherulites occurs at large undercooling whereas the formation of axialites due to incomplete splaying occurs at lower undercoolings.

In the case of blends, the splaying of lamellas occurs, but as pointed out by Keith and Padden,[5,6] a distinct change in lateral growth habit must occur. The reason outlined is that, in the case of blends, the impurities consisting of noncrystallizable or low molecular weight species are excluded from the growing crystals and consequently build up at growth fronts. If k is the growth rate of the front and D the diffusion coefficient of the rejected species, the diffusion length δ, which is a measure of segregation of the rejected species, is given by D/k. To allow for better dissipation of the rejected species, the growth front cellulates into fibrils of the size of δ. The cellulation of the lateral habit of the crystals with subsequent noncrystallographic branching was proposed to be sufficient for the formation of a full-fledged spherulite. Subsequent studies by Basset,[7−9] of morphology of homopolymers of broad molecular weight distribution, by etching of the spherulitic structure have shown no evidence of cell-like structures. As against cellulation there is clustering of the splaying lamellas into growth arms. The structure is more open, with segregation of the rejected species. This is in contrast to the homopolymer morphology, which is compact. A good example of this contrast is provided during the crystallization of isotactic polystyrene (i-PS) and blends of isotactic and atactic polystyrene (a-PS).[10] Two morphologies of crystallization exist as a function of the undercooling in the blend. At low undercoolings, the structures observed are as sketched in Figure 2 and represent the transition of a compact axialite/hedrite to a more open one with the formation of growth arms.

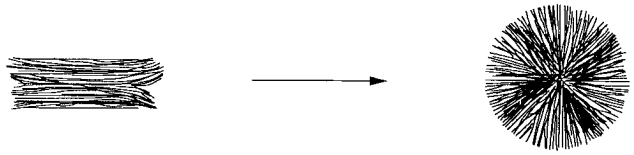

Figure 1. Growth of a compact spherulite of homopolymer from sheaf structures.

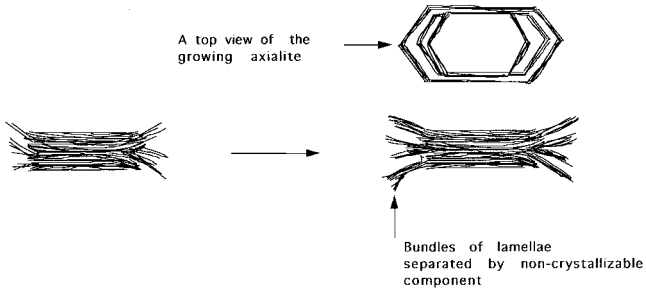

Figure 2. Growth of an open sheaf structure at low undercoolings for blends.

[⊗] Abstract published in *Advance ACS Abstracts,* February 1, 1996.

0024-9297/96/2229-2095$12.00/0

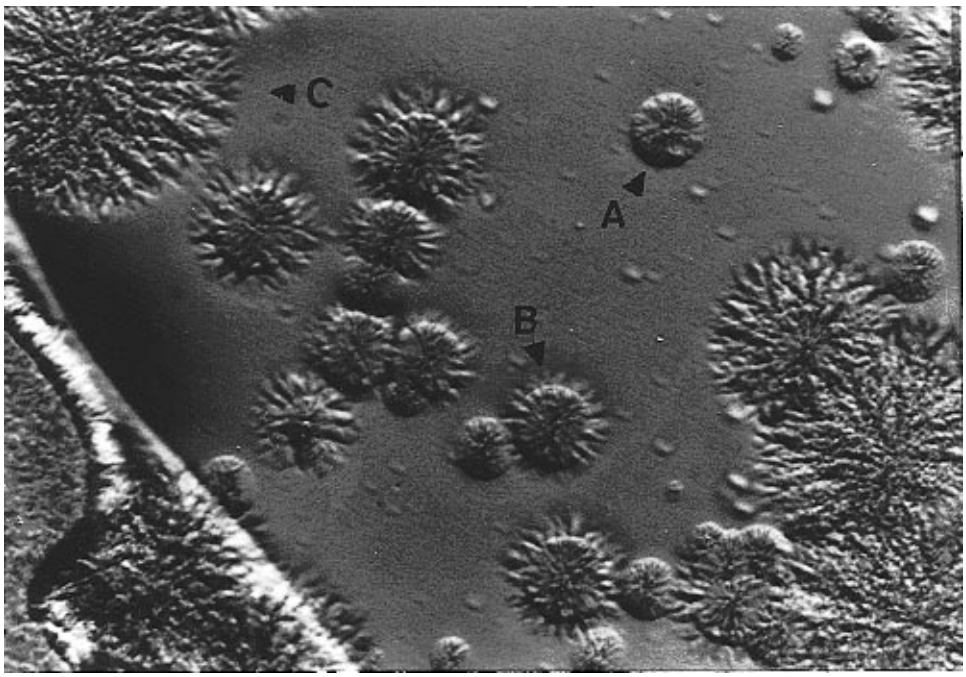

Figure 3. Growth of an open spherulite from a compact spherulite at higher undercoolings: (A) A compact spherulite of poly(aryl ether ketone ketone). (B) Breakdown of the spherulite at a critical radius. (C) Growth of an open structure after breakdown of the interface.

At higher undercoolings, the structures are mature spherulites with bundles of lamellas separated by atactic component. Recent work on crystallization of poly(aryl ether ketone ketone) (PEKK) of broad molecular weight distribution shows this transition from a compact spherulite to a more open one, as in Figure 3.[11] Figure 2 would represent the clustering of lamellas occurring before splaying to a complete three-dimensional spherulite and Figure 3 would be the opposite case. It is our contention that the transition from compact to more open structures with distinct growth arms is due to the segregation of impurities and that the splaying of axialites/hedrites to spherulites, common to both homopolymer and blend morphologies, is independent of impurities.

In this paper we address the formation of open spherulites from compact ones as in Figure 3, which occurs at higher undercoolings. Specifically, we would like to predict the radius of the spherulite at which the transition occurs. The transition is treated as a shape stability of a growing crystal. As the spherulite grows it rejects the low molecular weight or atatic species (referred to as solute species). At some stage, the growth rate of the interface is faster than the rate at which the solute species can diffuse away. To allow for better dissipation of solute, the interface breaks down. In terms of a formal theory of stability of growth, the earliest work on this subject goes back to the classical work of Mullins and Sekerka.[12] The growth of a perturbation on a sphere is favored by the gradient in the diffusion field of the solute, such that any protrusion of the crystal beyond the mean interface would be in a position to collect more material. The growth of such protrusions would be dampened by a capillarity effect of the interface surface energy, which acts to restore the original interface. A balance between the two effects gives us the critical radius of instability of a growing sphere. Subsequently, Coriell and Parker[13] included the effect of linear kinetics of attachment at the interface for growth of a sphere in a thermal field. The results were translated to the case of a growing polymer sphere in a solutal field by Calvert.[14] In many cases a stable interface was predicted.

In this work we consider the growth of a compact sphere with the assumptions that (1) solute is wholly rejected at the interface, (2) the solute does not alter the melting point and the mobility of the crystallizing species, and (3) the solute does not alter the work required to form the nucleus of the crystallizing species. The Lauritzen and Hoffman kinetic growth rate, corrected for the presence of the solutal field, is assumed at the interface. A perturbation of the growing sphere in the form of a spherical harmonic is introduced and the critical radius of instability computed at the point where the perturbation grows at least as fast as the sphere itself. The critical radius of instability of the growing sphere as a function of the undercooling, solutal composition and the diffusivity of the solute have been computed. Results for the case of blends of i-PS and a-PS indicate that there exists a sharp transition from relatively stable spheres to unstable spheres over a few degress of undercooling. At large undercoolings, the size of the stable sphere is in the submicrometer range and changes relatively slowly with the degree of undercooling. The critical radius of the sphere provides an upper bound for the formation of bundles in a spherulite of the blend, based on interfacial instability, in turn, by diffusion limitations of the solute. The value of the upper bound is consistent with experimental results on (a) the magnitude of the bundle size and (b) the relative constancy of the bundle size in the range of large undercoolings. The critical radius of instability is also a function of the spherical harmonic, showing a minimum with respect to the harmonic number. The harmonic number is intrepreted as the degree of branching. A high harmonic number would be a high degree of branching, which would in turn mean a comparatively compact structure, whereas a low harmonic number would mean a relatively open structure. Results of the analysis indicate that, at lower undercoolings and high diffusivities, a high degree of branching is expected and vice versa.

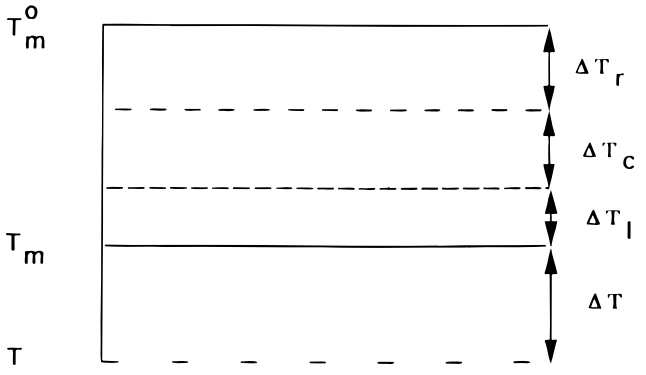

Figure 4. Depression in melting point of the crystallizing species.

Problem Formulation

(1) Kinetics of Attachment. Consider the growth of a compact sphere consisting of radial arrays of lamellar crystallites. Polymer chains go from the melt to the lamellar crystals by chain folding onto a fold surface. Growth occurs by secondary nucleation of new molecular layers on the growing surface of a crystallite. The largest barrier to the nucleation is the addition of the first stem. Considering an average length of the crystallizing stem, the work required for its formation can be expressed as[15]

$$\langle \Delta F \rangle = \frac{4 b_0 \langle \sigma \sigma_e \rangle}{\Delta f_v} \tag{1}$$

Here, σ and σ_e are the energies per unit area parallel and perpendicular to the molecular chain direction. The quantities between brackets represent average quantities. Here, b_0 represents the thickness of an added stem and Δf_v is the bulk free energy of fusion, defined as

$$\Delta f_v = \frac{\Delta h_f (T_m - T)}{T_m} \tag{2}$$

where T_m is the equilibrium melting point and T is the local temperature of the melt. The difference between T_m and T is the undercooling, which provides the driving force for growth. The local T_m for a polymer melt can be deduced from the corrections to the equilibrium melting point of a polymer chain of infinite length, defined as T_m^0. In Figure 4, ΔT_l is the correction if the chain length is finite, ΔT_r is the correction of the melting temperature in going from a bulk phase to one that has a curved interface, and ΔT_c is the correction due to the presence of solute. Here, we neglect the effect of chain length and the presence of solute on the equilibrium melting point. The local equilibrium temperature corrected only for the curvature effect is given by the Gibbs−Thompson relation:

$$T_m = T_m^0 - \Gamma_R \kappa \tag{3}$$

$$\Gamma_R = \frac{2 \sigma_r T_m^0}{\Delta h_f} \tag{4}$$

Here, σ_r is the surface energy of the melt/crystal interface, Δh_f is the heat of fusion in calories per cubic centimeter, and κ is the local curvature of the interface. The growth rate based on interface kinetics is thus

$$k = \beta \exp\left[- \frac{\Delta F}{k_B T} \right] \tag{5}$$

where k_B is Boltzmann's constant and β is the transport rate of segments across the interface. Substituting eq 2 into eq 1 and eq 1 into eq 5, the growth rate is given by

$$k = \beta \exp\left[- \frac{K_g^0 T_m}{T T_m^0 (T_m - T)} \right] \tag{6}$$

where K_g^0 is defined by

$$K_g^0 = \frac{4 b_0 \langle \sigma \sigma_e \rangle T_m^0}{\Delta h_f k_B} \tag{7}$$

The growth rate is corrected for the presence of the solute species and is taken to be proportional to the volume fraction v_2 of the crystallizing species.[16] If the densities of the solute species and the crystallizing species are equal, then $v_2 = \omega_2 = 1 - \omega_1$, where ω_1 is the weight fraction of the solute species and ω_2 that of the crystallizing species. The net velocity of growth of the front is given by

$$\frac{dR}{dt} = (1 - \omega_1) k \tag{8}$$

where R is the radius of the growing sphere.

(2) Conservation of Solute Field. Ahead of the growing envelope of the tiny sphere we can write the conservation of the solute species. We use Laplace's equation in place of the time-dependent diffusion equation. This would be true if the rate of growth of the sphere is slower than the diffusive process in the bulk. The net rate of pileup of the solute is characterized by the diffusion length, D/k, where D is the center-of-mass diffusivity. If the diffusion length is much greater than R, then the solute profile ahead develops slowly and the Laplace equation is assumed to apply. The relevant parameter would be the Peclet number (Pe) defined as kR/D. This restricts our treatment to $Pe \ll 1$.

$$\nabla^2 \omega_1 = 0 \tag{9}$$

$$r = \infty, \quad \omega_1 = \omega_\infty \tag{10}$$

The conservation conditions at the interface for the case where the solute is wholly rejected from the growing sphere is

$$\omega_i \frac{dR}{dt} = -D \frac{\partial \omega_1}{\partial r} \tag{11}$$

$$r = R, \quad \omega_1 = \omega_i \tag{12}$$

Combining eqs 8 and 11, the conservation of the solute species is

$$\frac{dR}{dt} = - \frac{D}{\omega_i} \frac{\partial \omega_1}{\partial r} = k(1 - \omega_i) \tag{13}$$

where ω_i is the concentration of solute in the melt at the interface. Equations 9, 10, 12, and 13 represent the growth of the polymer sphere under kinetics of attach-

ment of the crystallizing species and diffusion of the solute species.

Stability Analysis

Consider now the process of growth of a compact sphere by crystallization from an undercooled melt. When the sphere is tiny, the radius of curvature is large and most of the driving force (which is the undercooling) goes to creating a surface of high curvature. The growth rate is slow. As the tiny sphere grows, the radius of curvature decreases and the growth rate increases. At the same time, the growing spherulite rejects the solute species. The pileup of the rejected species decreases the kinetic growth rate as there is a smaller concentration of the crystallizable species at the interface. At some radius level the driving force available would be greater than the slowed growth due to solute pileup. The system then tries to find an optimum way of dissipating the solute ahead of it. The spherical interface becomes unstable to perturbations and decomposes into lamellar protuberances. Qualitatively any protuberance of the interface is in a position to collect more of the crystallizable species and grow faster than the base. The scale of the perturbation is however limited by the capillary forces which tend to dampen the growth. A balance of the two effects determines the size of the sphere, which is at its point of instability. For the case of a compact spherulite, the nature of the perturbation is necessarily an increase in the surface area of the crystal/amorphous interface. We investigate the behavior of this infinitesimally distorted sphere caused by a single harmonic, $Y_{l\mathrm{m}}$. The equation of the surface of a distorted sphere is given by

$$R' = R + \delta Y_{l\mathrm{m}} \tag{14}$$

where δ is very small compared to the radius of the sphere. The local curvature of the interface is given by[12]

$$\kappa = \kappa_0 + \frac{(l-1)(l+2)\delta Y_{l\mathrm{m}}}{R^2} \tag{15}$$

$$\kappa_0 = 2/R \tag{16}$$

For small deviations of κ from κ_0, the kinetic growth rate k in eq 6 can be expanded in a Taylor series about $\kappa_0 = 2/R$

$$k(\kappa) = k_0(\kappa_0)\left[1 + \frac{\alpha^*(\kappa_0)(l-1)(l+2)\delta Y_{l\mathrm{m}}}{R^2}\right] \tag{17}$$

$$\alpha_*(\kappa_0) = [\partial k/\partial\kappa]_{\kappa=\kappa_0} \tag{18}$$

Here k_0 is the Lauritzen and Hoffman rate of kinetics of attachment given by eq 6 when the curvature correction to the melting point is for an unperturbed sphere of curvature $\kappa_0 = 2/R$. For the sake of the stability analysis it is enough to note that k_0 and α^* are functions of $\kappa_0 = 2/R$. The interface concentration and the gradient in concentration for the solute species are given to a first order in δ as[17]

$$\omega_i = \omega_\infty + \frac{a}{R} + \left(\frac{b}{R^{l+1}} - \frac{a}{R^2}\right)\delta Y_{l\mathrm{m}} \tag{19}$$

$$-(\nabla\omega)_{\mathrm{r=R'}} = \frac{a}{R^2} - \left(\frac{2a}{R^3} - \frac{(l+1)b}{R^{l+2}}\right)\delta Y_{l\mathrm{m}} \tag{20}$$

The profile chosen satisfies the Laplace equation (9) and reduces to the proper value of $\omega_i = \omega_\infty$ far away from the interface. Substituting equations for k, ω_i, and $\nabla\omega$ into the conservation condition given by eq 13 and retaining terms of order δ to determine the parameters a and b, we have a as given by

$$a = Rf[Pe(R),\omega_\infty] \tag{21}$$

where f is given by

$$f[Pe(R),\omega_\infty] = \frac{-\left[\frac{1}{Pe(R)} + (2\omega_\infty - 1)\right] + \sqrt{\left[\frac{1}{Pe(R)} + (2\omega_\infty - 1)\right]^2 + 4\omega_\infty(1-\omega_\infty)}}{2} \tag{22}$$

Here, the Peclet number $Pe(R) = k_0R/D$. The parameter b in turn is given by the expression,

$$\frac{b}{R^{l+1}} = \frac{G_1 + G_2}{G_3} \tag{23}$$

where G_1, G_2, and G_3 are given by

$$G_1 = \left[\frac{2a}{R^2(\omega_\infty + a/R)} - \frac{a^2}{R^3(\omega_\infty + a/R)^2} + \frac{aPe(R)}{R^2}\right] \tag{24}$$

$$G_2 = \left[\frac{\alpha^*Pe(R)(1-\omega_\infty)(l-1)(l+2)}{R^2} - \frac{a\alpha^*Pe(R)(l-1)(l+2)}{R^3}\right] \tag{25}$$

$$G_3 = \left[(\omega_\infty + a/R) - \frac{a}{R(\omega_\infty + a/R)^2} + Pe(R)\right] \tag{26}$$

The radial growth of the infinitesimally perturbed sphere is given by

$$\frac{\mathrm{d}R}{\mathrm{d}t} + \frac{\mathrm{d}\delta}{\mathrm{d}t}Y_{l\mathrm{m}} = -\frac{D}{\omega_{\mathrm{i}}}\left(\frac{\partial\omega_{\mathrm{i}}}{\partial r}\right)_{\mathrm{r=R'}} = \frac{D}{(\omega_\infty + a/R)}\left[\frac{a}{R^2} - \left(\frac{2a}{R^3} - \frac{(l+1)b}{R^{l+2}}\right)\delta Y_{l\mathrm{m}} - \frac{a}{R^2(\omega_\infty + a/R)}\left(\frac{b}{R^{l+1}} - \frac{a}{R^2}\right)\delta Y_{l\mathrm{m}}\right] \tag{27}$$

Equating like coefficients, the growth of the undistorted sphere and the growth of the perturbation are given as

$$\frac{\mathrm{d}R}{\mathrm{d}t} = \frac{D}{(\omega_\infty + a/R)}\frac{a}{R^2} \tag{28}$$

$$\frac{1}{\delta}\frac{\mathrm{d}\delta}{\mathrm{d}t} = k_0(R)\left[\left(\frac{a}{R^2} - \frac{b}{R^{l+1}}\right) + \frac{\alpha^*(1-\omega_\infty)(l-1)(l+2)}{R^2} - \frac{\alpha^*(l-1)(l+2)}{R^3}\right] \tag{29}$$

The growth of the undistorted sphere is a function of the radius of the sphere, and the growth rate of the perturbation is a function of the radius of the sphere and the spherical harmonic. For $l = 1$, it can be shown from eq 29 that $\mathrm{d}\delta/\mathrm{d}t = 0$ and is a result of the fact that the $l = 1$ harmonic only translates the sphere and does

not perturb it. We now define the relative stability criterion of the growth of a perturbation as

$$\left(\frac{\mathrm{d}\ln\delta}{\mathrm{d}t}\right)\Big/\left(\frac{\mathrm{d}\ln R}{\mathrm{d}t}\right) = 1 \tag{30}$$

The relative stability criterion defines the radius of the sphere at which a critical perturbation grows at least as fast as the sphere itself. It can be shown that for the harmonic $l = 2$ the perturbation diminishes relative to the size of the sphere. Consequently, the harmonics that satisfy the criteria given by eq 30 are for $l \geq 3$. Utilizing eqs 28 and 29, the relative radius of stability, R_r, is given by

$$R_r = \frac{[-L_1(L_\alpha - D/k_0) + \sqrt{L_1^2(L_\alpha - D/k_0)^2 + 4L_\alpha L_1(1-\omega_\infty)R_r/f}]}{2} \tag{31}$$

$$L_1 = \frac{[l + \omega_\infty/(\omega_\infty + f)]}{(l-2)(\omega_\infty + f)} \tag{32}$$

$$L_\alpha = -\alpha^*(l+2)(l-1)(\omega_\infty + f) \tag{33}$$

The equation for R_r is a transcendental equation and has to be solved iteratively as a function of the spherical harmonic for specified far-field composition ω_∞ and undercooling. The results of this section which are relevant to our interest are the velocity of growth of the undistorted sphere, given by eq 28 and the relative radius of stability predicted by eq 31. In the next section these properties are examined for the case of a polymer blend.

Results

The velocity of growth of the undistorted sphere is given by eq 28 of the stability analysis. The complete equation for growth is not illustrative in the present form. We look at the original eq 8 in the case where $\kappa = \kappa_0$. The equation can be manipulated to the more illuminating form

$$\frac{\mathrm{d}R}{\mathrm{d}t} = k_\infty \exp\left[-\frac{l^*}{(R - R^*)}\right](1 - \omega_i) \tag{34}$$

$$l^* = \left[\frac{K_g^0}{T_m^0(T_m^0 - T)}\right]R^* \tag{35}$$

$$k_\infty = \beta \exp\left[-\frac{K_g^0}{(T_m^0 - T)}\right] \tag{36}$$

Here l^* is the length of the surface created due to the kinetic process of attachment in terms of the capillarity length $R^* = 2\Gamma_r/(T_m^0 - T)$. Here, k_∞ is the Lauritzen and Hoffman growth rate of the homopolymer. Initially when the sphere is small the curvature is high and growth rate is slow, as reflected by the second term of the right-hand side of eq 34. As the sphere becomes larger the curvature decreases, but the amount of solute species piling up ahead of the interface increases as reflected by the third term of the equation. The net result is that the growth rate goes through a maximum. For the case of a blend of i-PS and a-PS, the relevant kinetic and diffusional parameters are given in Table

Table 1. Kinetic and Thermodynamic Parameters of Crystallization of i-PS

Kinetic Data[19]

$M_w = 2.2 \times 10^6$	$U^* = 1560$ cal/mol
$T_m^0 = 515.2$ K	$K_g = 1.2 \times 10^5$ K^2
$T_0 = 335.5$ K	$\beta = A_f \exp\left[-\frac{U^*}{R_q(T - T_0)}\right]$
$A_f = 2.7 \times 10^{-2}$ cm/s	

Thermodynamic Data[20]

$\rho = 1.04$ g/mL	$\sigma_r = 10^{-7}$ cal/cm^2
$\Delta h_f = 2150$ cal/mol repeat unit	

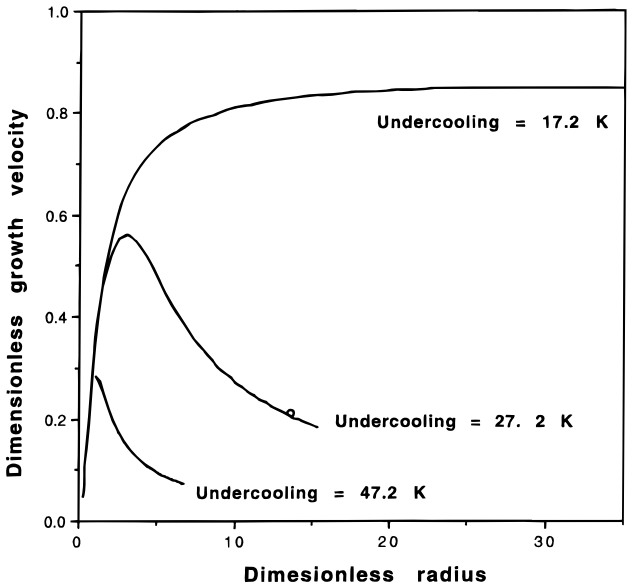

Figure 5. Velocity of growth of a sphere as a function of its radius. The velocity is scaled with k_∞ and the radius with l^*. Here $\omega_\infty = 0.1$ and $D = 10^{-13}$ cm^2/s.

1. The calculated growth rate is plotted in Figure 5. The radius of the sphere is scaled with l^* and the velocity of the sphere is scaled with k_∞, the growth rate of the homopolymer. The plot at first seems unusual, given the constant growth rates observed by optical microscopy. The scale of the radius of the growing sphere is however important in interpreting the plot. For a dimensionless radius of 10 in the graph, the actual size of the sphere is about 0.3 μm for an undercooling of 27.2 K. At radii smaller than this, the growth of a condensed phase should be limited by capillarity effects, that is, at very small radii, most of the undercooling goes toward maintaining a capillarity limited spherical surface. The resulting velocity is small. As the sphere grows larger, capillary effects diminish and the growth velocity increases. This behavior would be hard to see experimentally by optical microscopy, given the small radii. The consequent decrease of the growth velocity is clearly due to the pileup of the solute ahead of the sphere; i.e., growth becomes diffusion limited. However, this does not happen for long, before the velocity of the sphere decreases to a point where there is excess driving force available, but the sphere cannot grow faster due to diffusional limitations of the solute. At this point the interface breaks down into lamellar protuberances. The lamellar protuberances represent a geometry that dissipates solute faster and also grow at a steady velocity, representative of constant spherulitic growth rates observed in blends.

The relative radius of stability for a perturbed sphere is given by eq 31 and is a function of the spherical harmonic. Figure 6 is the R_r predicted at two different

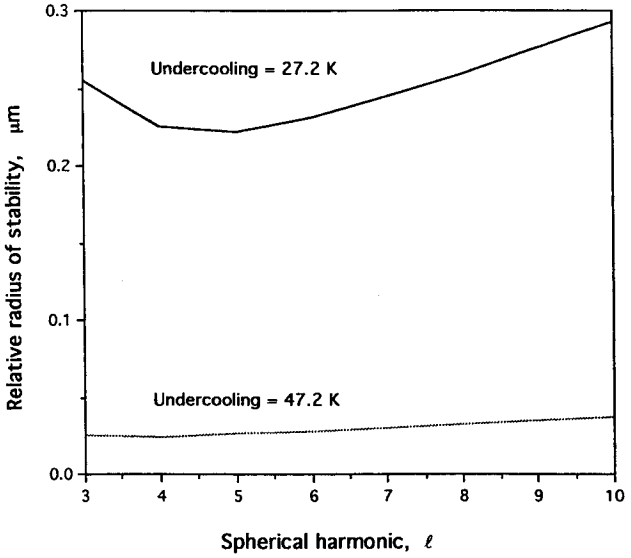

Figure 6. Relative radius of stability of the sphere as a function of the harmonic number. Here $\omega_\infty = 0.1$ and $D = 10^{-13}$ cm^2/s.

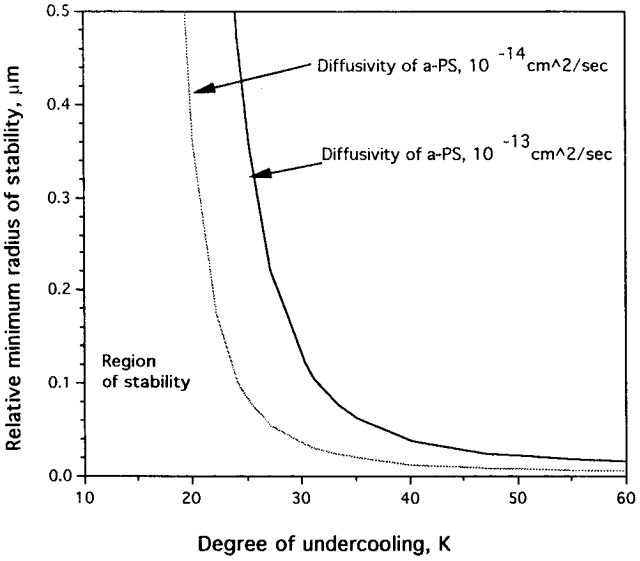

Figure 7. Neutral stability curve of the critical radius of stability as a function of the undercooling. Here $\omega_\infty = 0.1$.

undercoolings. The plot shows a minimum with respect to the harmonic number. At higher harmonics we have a large number of undulations, in which case the restorative effect of capillarity is large. At lower harmonics the surface is shallow, resulting in the tip and the base of the undulation essentially seeing the same concentration of the solute species, rendering the sphere stable. The critical radius is given by a radius corresponding to l_{min}. The radius corresponding to the minimum value is picked for each undercooling, and the neutral stability curve is constructed in Figure 7. Figure 7 is a plot of the critical radius of instability as a function of the undercooling. The plot is to be interpreted as follows: at an undercooling of 25 K all spheres of radius >0.4 μm are unstable for an a-PS diffusivity of 10^{-13} cm^2/s. At large undercoolings (35−55 K) the R_r predicted are in the range of 0.06−0.02 μm for an atactic diffusivity of 10^{-13} cm^2/s. There is a relatively slow change in the predicted R_r's with undercooling. The plot also shows that there is a relatively sharp transition from large stable spheres to small unstable ones over a few degrees of undercooling, e.g.,

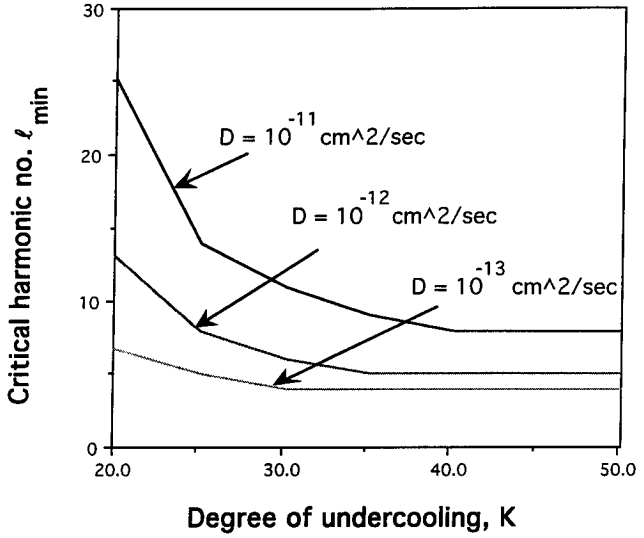

Figure 8. Critical harmonic number as a function of the undercooling and diffusivity of the solute species. Here $\omega_\infty = 0.1$.

from 17 to 20 K for an a-PS diffusivity of 10^{-13} cm^2/s. The transition can be easily rationalized from the standpoint of the polymer kinetic growth law. The kinetic growth rate is of the form $\exp[-1/\Delta T]$, where ΔT is the undercooling. Consequently, the velocity of growth increases exponentially with the undercooling and the critical radius of stability shows the opposite trend with undercoolings, consistent with the fact that faster growing interfaces break down earlier compared to slower growing interfaces. It is of interest to locate the point of critical radius of instability on the velocity vs radius curve in Figure 5. This point is marked as a circle for an undercooling of 27.2 K. The point of breakdown occurs when the growth is severly limited by the diffusivity of the solute.

Another useful result can be deduced from Figure 8, a plot of the critical harmonic number l_{min} as a function of the undercooling and diffusivity of the atactic species. At low undercoolings, the least stabilized harmonics are the higher ones; i.e., the surface needs to be sharply undulated to cause appreciable differences in the concentration of the crystallizable species between the tip and the base of the perturbation to cause instability. At higher undercoolings, the growth velocity is high and the solute pileup in front of the interface is large. Only small undulations are needed to see a difference in the concentrations at the tip and the base of the perturbation to cause growth. The critical harmonic number can be interpreted as the initial degree of branching; the analysis shows that at low undercoolings we should have a large stable sphere, which breaks down into many lamellar protuberances, characterized by a large value of the critical harmonic number. The transition is that of a compact sphere to a structure that is relatively compact due to the large number of protuberances. At high undercoolings, the analysis predicts a breakdown of a small sphere into a small number of harmonics. The transition is that of a compact sphere to a more open structure due to the smaller number of protuberances. The critical harmonic number is a strong function of the diffusivity of the solute. At a fixed undercooling, the faster diffusion promotes a shallow concentration profile, requiring that the interface be sharply undulated for unstable growth. Consequently, high diffusivity of the solute leads to compact structures

Table 2. Comparison of Experimental Data[10] of Measured "Fibril" Diameter with Predictions of the Model for a 50:50 Blend of i-PS/a-PS ($\omega_\infty = 0.5$)

T (°C)	D (cm²/s)	R_r (μm)	l_{min}	λ_{theor} (μm)	λ_{expt} (μm)[10]
190	1.37×10^{-11}	0.65	8	0.51	0.1
210	2.43×10^{-10}	57	25	14.3	<0.5

and low diffusivities of solute species to sparse structures. The variation of l_{min} with blend composition is, however, not significant. It should be noted that the prediction for the critical number of harmonics is only at the point of instability, i.e., at an early stage of growth of the spherulite.

Discussion

The results of the analysis are compared to the experimental results of Vaughan on the crystallization of isotactic/atactic polystyrene (i-PS/a-PS) blends.[10] Vaughan's results are as follows: (1) Above 200 °C i-PS of $M_w = 8.4 \times 10^5$ crystallized in sheaflike morphologies, as sketched in Figure 1. (2) Reducing the temperature below 200 °C resulted in compact structures whose envelope is almost spherical. (3) Addition of a-PS to the extent of 50% by weight of $M_w = 2.3 \times 10^5$ resulted in open structures. (4) Above 200 °C, the structures were sheaflike but with clustering of lamellas into growth arms, as sketched in Figure 2. (5) Below 200 °C, the structures were mature spherulites with bundles of lamellars separated by atactic component. The results of the analysis are compared for temperatures of crystallization below 200 °C only, where we can expect a transition from a compact sphere to an open one with the formation of bundles of crystallites. The formation of these bundles in the blend is due to the growth front of the spherulite adopting a better dissipative geometry. The process occurs through a transition of a compact growing sphere to a more open one. Direct observation of the transition as predicted by the analysis at the temperatures of interest for the i-PS/a-PS blend system is in the submicrometer range and would be difficult to observe experimentally. However, to check the validity of the model, we compare the wavelength of the perturbation ($\lambda = [2\pi/l_{min}]R_r$) at the onset of breakdown with the diameter of the lamellar protuberances observed in the spherulite. The comparison entails that the final diameter of the bundles achieved by the spherulite is also a diffusion-limited process. The wavelength then provides an upper bound to the bundle size. The results of the analysis are compared to the experimental results of Vaughan[10] in Table 2. The kinetic and thermodynamic parameters are listed in Table 1. The diffusivity of a-PS, of the same molecular weight as i-PS, is assumed to be the self-diffusivity of the polymer, and its value is reduced from the data of Whitlow and Wool[18] (the diffusivity of polystyrene of molecular weight $M_w = 1.99 \times 10^5$ is given by $D = D_0 \exp[-Q/RT]$, where $Q = 64.2$ kcal/mol and $D_0 = 1.768 \times 10^{19}$ cm²/s). The results match in the order of magnitude at a crystallization temperature of 190 °C. At this temperature, the structures observed were mature spherulites with growth arms separated by the atactic component. The critical harmonic number of the analysis indicates that the spherulite should be relatively open compared to the pure i-PS spherulite. The micrographs of Vaughan[10] agree qualitatively with this feature. At lower undercoolings (corresponding to a crystallizing temperature of 210 °C) the analysis is less valid. In this case, the structure is that of an axialite/hedrite with growth arms separated by the atatic component (as sketched in Figure 2). In fact, the predicted "fibril" diameter is here off by 2 orders of magnitude. Clearly, in such a case the idea of a fibril is incorrect, since the axialite/hedrite consists of stacks of hexagonal lamellar crystals with broad lamellar widths as compared to the thickness of the stack of the lamellas.[10] The pileup of solute is dictated by the largest dimension of the growing face of the hexagonal crystals. The transition from a compact axialite/hedrite to a more open one is associated with the clustering of the broad lamellas. The present analysis cannot predict the stack thickness in such a case. However, it is of interest to note the diameter of the stable sphere predicted at low undercoolings. The radius is about 57 μm, larger than the size of the hexagonal crystals observed in the axialites, which represent a stable morphology. This result is not entirely fortuitous but related to the fact that the transition to an unstable morphology has to occur when the size of the crystal is given by D/k, analogous to the growing sphere. However, the modulation of the interface is no longer spherically symmetrical in this case. In conclusion, the radius of transition predicted by the model for undercoolings of >25 K is in the submicrometer range. This is consistent with the fact that such transitions are difficult to observe experimentally and also consistent with the fact that the observed fibril or growth arm diameters in spherulites (not axialites) of blends are in the range of the wavelength of the perturbation at the point of transition.

Summary

The results of morphological stability of a polymer crystallizing from a binary melt have been examined for large undercoolings. It is shown that, for a polymer sphere crystallizing with its local interface kinetics and rejection of solute, there exists a transition from a compact sphere to a more open one at the point of morphological instability. The transition is shown to occur due to the diffusion limitations of the solute species. The radius of transition of the sphere is in the submicrometer range, consistent with the observed fibril diameters in blends of i-PS/a-PS. The radius of transition is also shown to remain relatively constant in the large undercooling region, which is also consistent with the observed experimental results.

Acknowledgment. We acknowledge the financial support by NSF under Grant DMR-9115308.

References and Notes

(1) Passaglia, E.; Khoury, F. In *Treatise on Solid State Chemistry*; Hannary, N. B., Ed.; Plenum: New York, 1976; Vol. 3, p 335.

(2) Vaughan, A. S.; Bassett, D. C. *Polymer* **1988**, *29*, 1397.

(3) Voigt-Martin, I. G.; Fischer, E.; Mandelkern, L., *J. Polym. Sci., Polym. Phys. Ed.* **1980**, *18*, 2347.

(4) Allen, R. C.; Mandelkern, L., *J. Polym. Sci., Polym. Phys. Ed.* **1982**, *20*, 1465.

(5) Keith, H. D.; Padden, F. J., Jr. *J. Appl. Phys.* **1963**, *34*, 2409.

(6) Keith, H. D.; Padden, F. J., Jr. *J. Appl. Phys.* **1964**, *35*, 1270.

(7) Bassett, D. C. In *Comprehensive Polymer Science*; Booth, C., Price, C., Eds.; Pergamon: Oxford, England, 1989; Vol. I, p 841.

(8) Vaughan, A. S.; Bassett, D. C. In *Comprehesive Polymer Science*; Booth, C., Price, C., Eds.; Pergamon: Oxford, England, 1989; Vol. II, p 415.

(9) Vaughan, A. S.; Bassett, D. C.; Olley, R. H. *Morphology of Polymers*; Walter de Gruyter: Berlin, 1986; p 387.
(10) Vaughan, A. S. *Polymer* **1988**, *33*, 2513.
(11) Wang, W.; Schultz, J. M., unpublished work.
(12) Mullins, W. W.; Sekerka, R. F. *J. Appl. Phys.* **1963**, *34*, 323.
(13) Coriell, S. R.; Parker, R. L. In *Crystal Growth*; Peiser, H. S., Ed.; Pergamon: Oxford, England, 1967; p 703.
(14) Calvert, P. D. *J. Polym. Sci., Polym. Lett. Ed.* **1983**, *21*, 467.
(15) Hoffman, J. D.; Lauritzen, J. I., Jr. *J. Res. Natl. Bur. Stds. (U.S.)* **1972**, *65A*, 297.
(16) Mandelkern, L. *Crystallization of Polymers*; McGraw-Hill: New York, 1964.
(17) Trivedi, R. *J. Cryst. Growth* **1980**, *48*, 93.
(18) Whitlow, S. J.; Wool, R. P. *Macromolecules* **1991**, *24*, 5926.
(19) Suzuki, T.; Kovacs, A. J. *Polym. J.* **1970**, *1*, 82.
(20) Tiller, W. A.; Schultz, J. M. *J. Polym. Sci., Polym. Phys. Ed.* **1984**, *22*, 143.

MA950904I